

Probing Cell Traction Forces in Confined Microenvironments

Phrabha S. Raman^{a‡}, Colin D. Paul^{a,b,c‡}, Kimberly M. Stroka^{a,b,c}, and

Konstantinos Konstantopoulos^{a,b,c,d*}

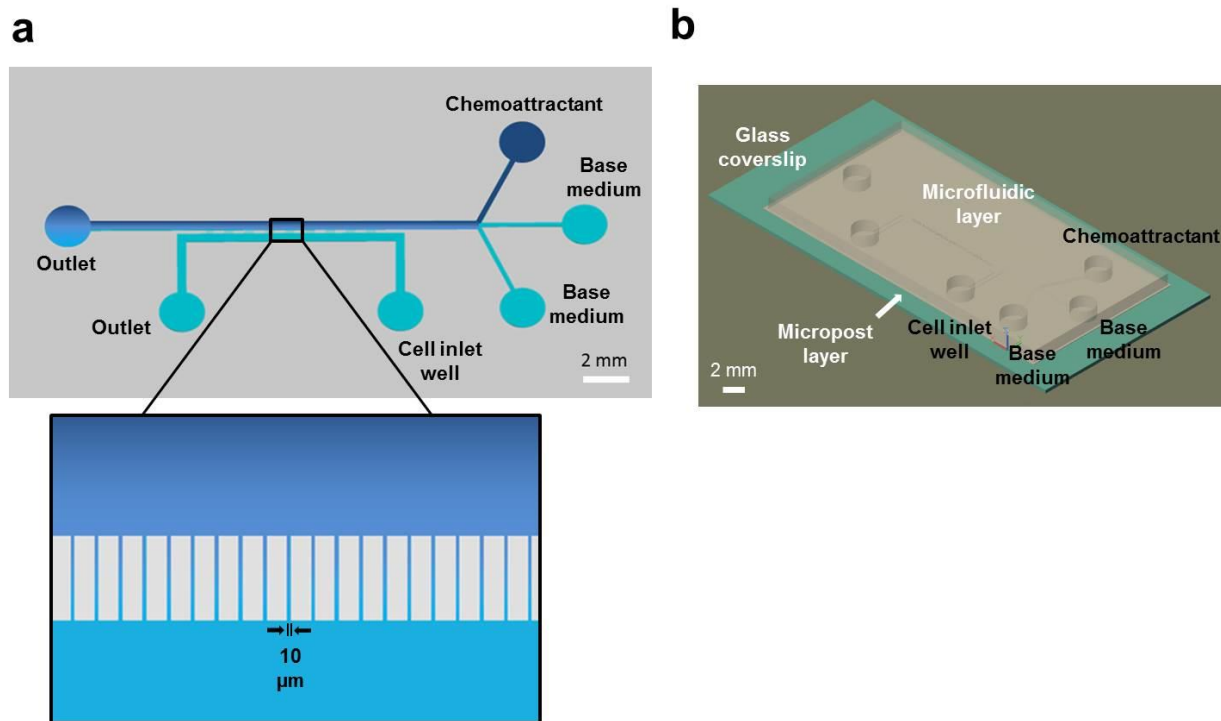
From ¹Department of Chemical and Biomolecular Engineering, ²Institute for NanoBioTechnology, ³Physical Sciences-Oncology Center, ⁴Center of Cancer Nanotechnology Excellence, The Johns Hopkins University, Baltimore, MD 21218, USA.

‡ These authors contributed equally to this work.

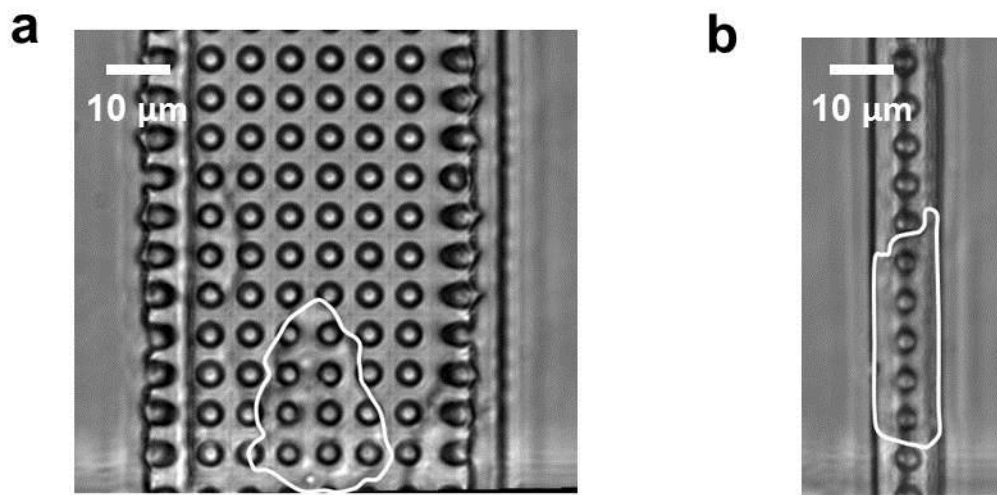
*To whom correspondence should be addressed:

Konstantinos Konstantopoulos, Ph.D.
Department of Chemical and Biomolecular Engineering
The Johns Hopkins University
3400 N. Charles Street
Baltimore, MD 21218
Tel: (410) 516-6290
Fax: (410) 516-5510
E-mail: konstant@jhu.edu

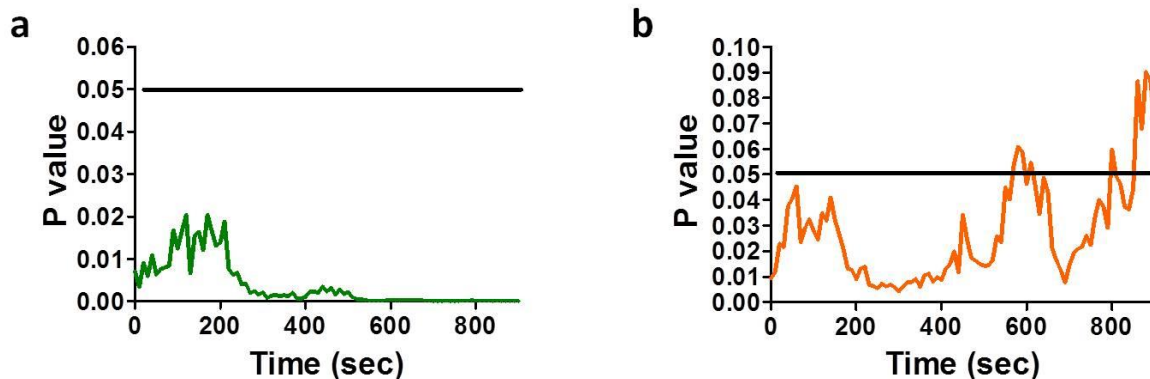
Supplementary Information



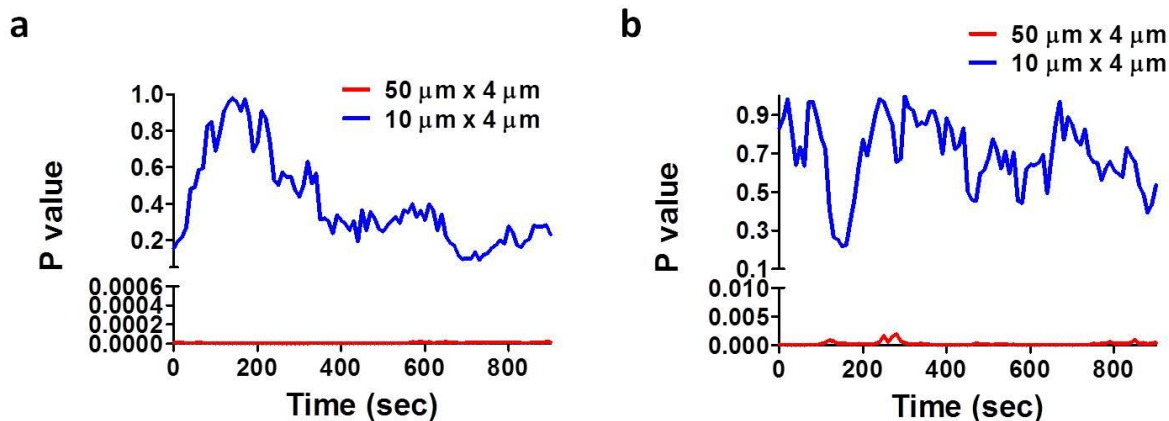
Supplementary Figure S1. (a) To-scale schematic of the microfluidic device. A chemoattractant gradient was generated within the 10, 20, or 50- μm wide, 4- μm tall microchannels by diffusion from a chemoattractant inlet port. Pressure-balanced laminar flow on each side of the microchannels minimized convective flow within the microchannels. Inlet ports for cell addition and insertion of chemoattractant-containing or base medium are indicated. Feed lines were 50 μm high. Inset shows a close-up of the chemoattractant gradient within the 10 μm -wide microchannels. (b) 3D rendering of the microfluidic device. Microposts were arrayed on a thin PDMS layer that was spin coated on a glass coverslip (micropost layer). A second PDMS layer defining the microchannels and microfluidic feed lines was aligned over the microposts (microfluidic layer). This layer contained vias for cell seeding and the addition of chemoattractant-containing or base medium to the device.



Supplementary Figure S2. Representative 40x magnification phase contrast images of HOS cells migrating through (a) unconfined and (b) confined microchannels encompassing an array of microposts at their bases. The width of microchannels is (a) 50 μm and (b) 10 μm. Cells are outlined for clarity.



Supplementary Figure S3. P values comparing average force per post magnitudes during unconfined ($50 \times 4 \mu\text{m}^2$) and confined ($10 \times 4 \mu\text{m}^2$) migration of (a) NIH-3T3 and (b) HOS cells at each time point over the duration of each experiment. P values were determined by two-tailed Student's t-test at each time point. P values beneath the horizontal black bar represents statistical significant differences between traction force exertion at that time point for cells in $50 \times 4 \mu\text{m}^2$ vs. $10 \times 4 \mu\text{m}^2$ microchannels.



Supplementary Figure S4. P values comparing average force per post magnitudes between control and drug-treated HOS cells migrating in $50 \times 4 \mu\text{m}^2$ and $10 \times 4 \mu\text{m}^2$ microchannels. Cells were treated with (a) 50 μM blebbistatin or (b) 0.1 nM calyculin A. P values were determined by two-tailed Student's t-test at each time point. In wide microchannels, treatment with blebbistatin resulted in significantly decreased force exertion ($P < 0.05$) at all time points, while calyculin A treatment resulted in significantly increased average traction forces ($P < 0.05$). Conversely, no significant differences ($P > 0.05$) in average traction forces were seen in narrow channels upon blebbistatin or calyculin A treatment.

Supplementary Video. Migration of (a) HOS cell within $20 \times 4 \mu\text{m}^2$ microchannel and (b) NIH-3T3 cell within $10 \times 4 \mu\text{m}^2$ microchannel. Microchannels contained an array of collagen type I-printed microposts at their bases, on which the cells migrated. Initial cell positions are outlined. Images were taken every 10 seconds using a 40x phase contrast objective. $20 \times 4 \mu\text{m}^2$ microchannels were not used for force measurement studies as cells were neither fully confined nor unconfined within these channels.